

Effects of flow shear on temperature gradient driven short wavelength modes

Zhe Gao^{a)}

Department of Engineering Physics, Tsinghua University, Beijing 100084, People's Republic of China

J. Q. Dong

Southwestern Institute of Physics, Chengdu 610041, People's Republic of China

H. Sanuki

National Institute for Fusion Science, Toki, Gifu 509-5292, Japan

(Received 30 December 2003; accepted 1 March 2004; published online 6 May 2004)

The effects of flow shear on the temperature gradient driven short wavelength ion (SWITG) modes and electron temperature gradient (ETG) modes are investigated in a sheared slab. The SWITG mode can be stabilized at arbitrary β when the $\mathbf{E} \times \mathbf{B}$ velocity shear, V_E' , reaches above a critical value. Since the SWITG mode has a lower frequency, a lower V_E' is needed to stabilize the SWITG mode than to stabilize the conventional ITG mode. However, the critical values of V_E' for stabilization of both SWITG and conventional ITG modes are much less than v_{ti}/L_n , where v_{ti} and L_n are ion thermal speed and the scale length of density gradient. Contrastively, the ETG mode cannot be stabilized until the V_E' is larger than v_{ti}/L_n . Similarly, a parallel velocity shear with order v_{ti}/L_n has significant effects on the SWITG mode but is too small to influence the ETG mode. The different behaviors of flow shear effects on the SWITG and ETG modes may indicate that the ETG mode is more reasonable than the SWITG as the candidate responsible for anomalous electron thermal transport. © 2004 American Institute of Physics. [DOI: 10.1063/1.1723422]

I. INTRODUCTION

Progress in understanding the anomalous transport in magnetically confined plasmas has been continuing for decades. It is now widely accepted that the anomalous transport is induced by turbulent plasma fluctuations with small scales, the so-called microinstabilities.¹ In particular, the temperature gradient (TG) driven instabilities are proposed as the plausible candidates responsible for anomalous thermal transport and have been studied extensively.^{2–11} Experimentally, many tokamaks have achieved reduced transport and enhanced confinement.^{12–16} The ion thermal diffusivity has been reduced to neoclassical level in advanced tokamak plasmas with internal transport barriers (ITBs). Strong sheared flows were usually observed accompanying the formation of transport barriers. Thus, the influence of sheared flow on plasma microinstabilities and turbulences has been one of the most interesting topics in recent decades.^{17–22} The model¹⁶ based on the $\mathbf{E} \times \mathbf{B}$ shear suppression effects on the ion temperature gradient (ITG) turbulence was developed to explain the transport reduction in enhanced confinement plasmas, since the measured $\mathbf{E} \times \mathbf{B}$ shearing rate exceeds the maximum linear growth rate of the ITG mode.^{23,24}

However, the electron transport continues to challenge our understanding. In many cases, the electron transport is still anomalous in discharges after the onset of the ITB. In the Joint European Torus (JET) experiments after the formation of an ITB, long wavelength (low-k) modes are suppressed, while short wavelength (high-k) modes are not.²⁵ It

is believed that the anomalous electron transport is governed by short wavelength turbulence, of course, after the stabilization of long wavelength turbulence. Recently, electron internal transport barriers (eITBs) have been reported in the presence of localized electron heating in both tokamaks^{26–30} and helical devices.³¹ However, it seems that the formation of eITBs is more likely to be triggered by the magnetic shear optimization rather than by the $\mathbf{E} \times \mathbf{B}$ shear enhancement. In DIII-D,³⁰ after onset of an eITB produced by ECH, fluctuation measurement indicates that both low-k and high-k turbulence are stabilized. However, the estimated $\mathbf{E} \times \mathbf{B}$ shearing rate is too small to suppress the high-k (ETG), and even the low-k (ITG-TEM) mode alone. There is also no evidence in other devices^{26–29} that the $\mathbf{E} \times \mathbf{B}$ shear suppresses the turbulence after the onset of the eITBs. The $s - \alpha$ stabilization^{32,33} is considered to explain the electron transport reduction, and other negative or weak magnetic shear effects also can influence the transport in many different ways.^{34–36}

Observation of electron temperature profile stiffness in experiments³⁷ indicates that the short wavelength instability responsible for electron transport is driven by finite electron temperature gradient. So, numerous studies have been performed on the electron temperature gradient (ETG) instabilities in recent years.^{38–41} The ETG mode in the electron diamagnetic direction ($\omega_r > 0$) is unstable in the very short wavelength region $k_y \rho_e \sim 1$. However, another unstable mode driven by temperature gradients in the short wavelength region $|k_y \rho_i| \gg 1$ is recently identified both in a slab^{42,43} and in a toroidal⁴⁴ configuration. This temperature gradient driven short wavelength ion (SWITG) mode propa-

^{a)}Electronic mail: gaozhe@mail.tsinghua.edu.cn

gates in the ion diamagnetic direction ($\omega_r < 0$) and requires both finite η_i and η_e for excitation. Although the growth rate of the SWITG mode is significantly smaller than that of the ETG mode, the cross-field wavelength of the SWITG mode is found to be much larger than that of the ETG mode. So the SWITG mode can produce a significant level of transport and should be paid more attention, especially in the presence of sheared flows.

In this paper, the integral equations⁴⁵ for the study of the ITG mode in the presence of sheared flows in arbitrary β plasmas are upgraded and then employed for the study of the SWITG mode in a sheared slab. The ETG mode is also studied with the same code. Then, a comparison between the flow shear effect on the SWITG mode and that on the ETG mode is given.

The organization of this paper is as follows. The extended integral eigenmode equations are presented in Sec. II. Numerical results and analyses are described in Sec. III. Section IV is devoted to conclusions and discussion.

II. INTEGRAL EIGENMODE EQUATIONS IN THE PRESENCE OF SHEARED FLOWS

We consider a sheared magnetic field $\mathbf{B} = B_0[\hat{\mathbf{z}}(1 + x/L_B) + \hat{\mathbf{y}}(x/L_s)]$, where L_s and L_B are the scale lengths of the magnetic shear and the magnetic gradient, respectively. The static equilibrium in a high β plasma slab requires a magnetic gradient: $L_n/L_B = \sum_{j=i,e}(\beta_j/2)(1 + \eta_j)$. Here, $L_n^{-1} = -(1/n_j)dn_j/dx$, $\eta_j = d \ln T_j/d \ln n_j$, and $\beta_j = 8\pi n_j T_j/B^2$. The general form of the equilibrium distributions in the presence of the parallel flow and the electric field $E(x)\hat{\mathbf{x}}$ can be written as⁴⁶

$$f_0 = g(X_g) \frac{n(X_g)}{\pi^{3/2} v_t^3} \exp \left[-\frac{v_x^2 + v_y^2 + (v_z - V_0)^2}{v_t^2} - \frac{q\Phi(x)}{T(X_g)} \right], \quad (1)$$

where $v_t = \sqrt{2T(X_g)/m}$, $E(x) = -\partial\Phi/\partial x$, $V_E = -cE(X_g)/B$, $V_0 = V_0(X_g)$, $X_g = x - (v_y - V_E)/\Omega$ is the radial coordinate of the guiding center and $\Omega = -qB_0/mc$ is the gyro-frequency. Here, the Ω_e is positive and this definition is consistent with the expression of X_g . The $g(X_g)$ is a function determined by the normalization condition, $\int f_0 d\mathbf{v} = n(x)$. Expanding the $\Phi(x)$ about X_g and substituting it into Eq. (1), the equilibrium distributions for ions and electrons are obtained as follows:

$$f_0 = h(X_g) \frac{n(X_g)}{\pi^{3/2} v_t^3} \exp \left[-\frac{v_x^2 + (v_y - V_E)^2 + (v_z - V_0)^2}{v_t^2} \right]. \quad (2)$$

As the second derivative of V_E is neglected, $h(X_g) = 1/(1 - V_E'/\Omega)$, which is just the reciprocal of the Jacobian determinant of the transformation from the lab coordinates to the guiding center coordinates. So the $g(X_g)$ can be eliminated by the coordinate transformation. The detailed procedure is well documented in Ref. 46 and will not be repeated here.

Expanding the sheared flows and neglecting the higher order derivatives, we obtain $V_0(x) = V_0(0) + V_0'x$, $V_E(x) = V_E(0) + V_E'x$. The flow velocities $V_0(0) = V_E(0) = 0$ are used, since the emphasis is placed on the effects of the flow shears, including the parallel velocity shear (PVS), V_0' , and the $\mathbf{E} \times \mathbf{B}$ velocity shear, V_E' . In this case the effects of a parallel flow and a toroidal flow should be equivalent. The effects of the parallel current and its gradient are not considered.

Three fluctuating scalar fields are introduced: $\tilde{\phi}$, \tilde{A}_\parallel ($= \tilde{\mathbf{A}} \cdot \mathbf{b}$), and \tilde{A}_2 ($= \tilde{\mathbf{A}} \times \mathbf{e}_\perp \cdot \mathbf{b}$), where all perturbed quantities have the form $\tilde{p}(\mathbf{r}, t) = p(x) \exp(ik_y y - i\omega t)$, $p(x) = 1/\sqrt{2\pi} \int p(k) \exp(ikx) dk$, $\mathbf{e}_\perp = \mathbf{k}_\perp / |\mathbf{k}_\perp|$, $\mathbf{k}_\perp = k_y \hat{\mathbf{y}} + k \hat{\mathbf{x}}$ and $\mathbf{b} = \mathbf{B}/B$. For the fluctuations with $\omega \ll |\Omega_j|$ and $k_\perp \lambda_d \ll 1$, we have derived⁴⁵ the kinetic integral equations for the study of the ITG mode at arbitrary β value. Replacing the quasineutrality condition with Poisson's equation in the previous equations, we get

$$\begin{aligned} \frac{k_\perp^2}{2} \frac{\Omega_e^2}{\omega_{pe}^2} \hat{\phi}(k) + \sum_j \frac{Z_j T_e}{T_j} \left\{ \hat{\phi}(k) \right. \\ \left. + \left(\frac{1}{2\pi} \right) \int dk' \int dx \exp[i(k' - k)x] \right. \\ \left. \times \left[L_j(0,0,0,0) \hat{\phi}(k') + \frac{v_{tj}}{v_{te}} L_j \left(0, 1, \frac{1}{2}, 0 \right) \hat{A}_2(k') \right. \right. \\ \left. \left. + \frac{v_{tj}}{v_{te}} L_j(0,0,0,1) \hat{A}_\parallel(k') \right] \right\} = 0, \quad (3) \end{aligned}$$

$$\begin{aligned} \hat{A}_2(k) - \sum_j \frac{\beta_j}{2\pi b_j} \left\{ \int dk' \int dx \exp[i(k' - k)x] \right. \\ \left. \times \left[\frac{v_{te}}{v_{tj}} L_j \left(1, 0, \frac{1}{2}, 0 \right) \hat{\phi}(k') + L_j(1,1,1,0) \hat{A}_2(k') \right. \right. \\ \left. \left. + L_j \left(1, 0, \frac{1}{2}, 1 \right) \hat{A}_\parallel(k') \right] \right\} = 0, \quad (4) \end{aligned}$$

$$\begin{aligned} \hat{A}_\parallel(k) - \sum_j \frac{\beta_j}{2\pi b_j} \left\{ \int dk' \int dx \exp[i(k' - k)x] \right. \\ \left. \times \left[\frac{v_{te}}{v_{tj}} L_j(0,0,0,1) \hat{\phi}(k') + L_j \left(0, 1, \frac{1}{2}, 1 \right) \hat{A}_2(k') \right. \right. \\ \left. \left. + L_j(0,0,0,2) \hat{A}_\parallel(k') \right] \right\} = 0. \quad (5) \end{aligned}$$

Here,

$$\begin{aligned} L_j(m, n, s, l) = \left(\frac{-q_j}{|q_j|} \right)^{m+n} \int_0^{+\infty} dt t^s \exp(-t) J_m(\sqrt{2b_j t}) \\ \times J_n(\sqrt{2b_j t}) \frac{\omega^{*j}}{\omega - \omega_{Dj} t} K_{lj}, \quad (6) \end{aligned}$$

$$\begin{aligned}
 K_{0j} = & \left(\frac{\omega_{0j}}{\omega_{*j}} - 1 \right) [\xi_j Z(\xi_j)] - \eta_j \left[\xi_j^2 + \left(\xi_j^2 - \frac{1}{2} \right) \xi_j Z(\xi_j) \right] \\
 & - \eta_j (t-1) [\xi_j Z(\xi_j)] + 2 \frac{L_n}{v_{tj}} \frac{\partial V_0}{\partial x} \frac{k_{\parallel}}{|k_{\parallel}|} \xi_j [1 \\
 & + \xi_j Z(\xi_j)] + 2 \frac{L_n}{v_{tj}} \frac{\partial V_E}{\partial x} \frac{ik'}{k'_{\perp}} \left[t^{1/2} \frac{-q_j}{|q_j|} \right. \\
 & \left. \times \frac{-J_n(\sqrt{2b'_j t})}{J_n(\sqrt{2b'_j t})} + \frac{\delta}{\sqrt{2b'_j t}} \right] \xi_j Z(\xi_j), \quad (7)
 \end{aligned}$$

$$K_{1j} = \frac{k_{\parallel}}{|k_{\parallel}|} \xi_j \left[K_{0j} + \left(\frac{\omega_0}{\omega_{*j}} - 1 \right) - \eta_j (t-1) \right], \quad (8)$$

$$K_{2j} = \frac{k_{\parallel}}{|k_{\parallel}|} \xi_j K_{1j}, \quad (9)$$

$\omega_{*j} = (k_y T_j) / (\Omega_j m_j L_n)$, $\omega_{Dj} = -\omega_{*j} L_n / L_B$, $b_j = k_{\perp}^2 \rho_j^2 / 2$, $b'_j = k_{\perp}^2 \rho_j^2 / 2$, $\rho_j = v_{tj} / \Omega_j$, $\xi_j = (\omega - \omega_{Dj} t) / |k_{\parallel}| v_{tj}$, $k_{\parallel} = (x/L_s) k_y$, $k_{\perp}^2 = k_y^2 + k_x^2$, $k_{\perp}^{\prime 2} = k_y^2 + k_x^{\prime 2}$, $\hat{\phi} = \phi$, $\hat{A}_2 = i v_{te} A_2 / c$, $\hat{A}_{\parallel} = -v_{te} A_{\parallel} / c$, and $Z(\xi)$ is the plasma dispersion function. In Eq. (6), δ equals one or zero when used in K_{0j} , depending on whether it is multiplied by \hat{A}_2 or by the other terms, respectively.

III. NUMERICAL RESULTS

The integral equations, Eqs. (3)–(5), are solved using the Raleigh–Ritz technique. The parameters are $\eta_e = 2$, $\eta_i = 2$, $T_e/T_i = 1$, $\Omega_e^2/\omega_{pe}^2 = 1$, and $m_i/m_e = 1836$ unless otherwise stated. The magnetic shear and poloidal wavenumber parameters are chosen differently: $L_n/L_s = 0.025$ and $k_y \rho_e = 0.1$ for SWITG modes and $L_n/L_s = 0.1$ and $k_y \rho_e = 0.8$ for ETG modes, approximately corresponding to the maximum growth rate of the two kinds of mode, respectively. When the effect of the PVS is examined, the $\mathbf{E} \times \mathbf{B}$ velocity shear is null and *vice versa*. The dimensionless flow shear parameters are $\hat{V}'_0 = L_n V'_0 / v_{ti}$, $\hat{V}'_E = L_n V'_E / v_{ti}$ and the wavelength is normalized to ρ_e^{-1} .

Shown in Fig. 1 are the k_y spectra of the SWITG modes for different \hat{V}'_0 values. In the small k_y region, the SWITG-PVS mode couples to the conventional ITG-PVS mode and the V'_0 is strongly destabilizing. As the k_y increases, the destabilizing effect of V'_0 on the mode is weakening, and even the V'_0 reverses to be stabilizing the mode after $k_y \rho_e > 0.4$. However, the effect of the PVS is dramatically reduced at a high β ($\beta_e \sim 5\%$). The real frequencies and growth rates of the SWITG modes are shown in Fig. 2 as functions of \hat{V}'_0 for different β values. This behavior is similar to that of the conventional ITG.⁴⁵ Also, the PVS destroys the symmetry in mode structure. Figure 3 shows that the mode structure shifts toward the $+x$ direction at a positive \hat{V}'_0 , which is common physics even when the mode under consideration is different.^{45,47}

The real frequencies and growth rates of the ETG modes are also shown in Fig. 4 in the presence of V'_0 for different β values. The V'_0 with order v_{te}/L_n can significantly destabilize the ETG modes just as the V'_0 with order v_{ti}/L_n does for

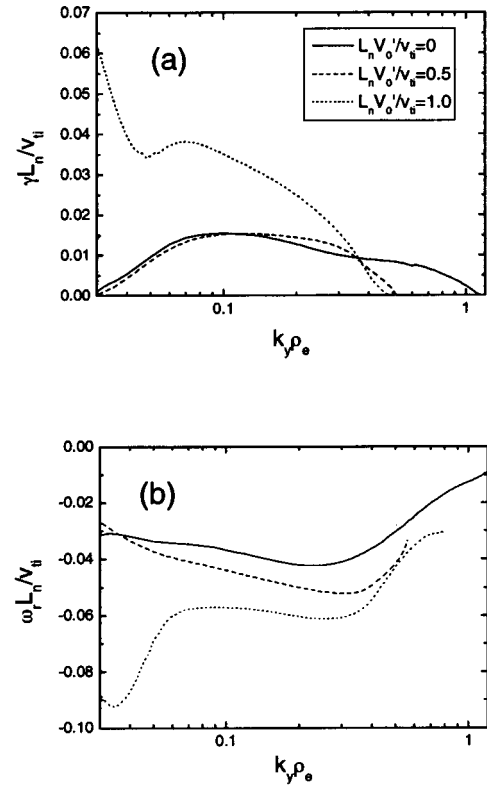


FIG. 1. Mode growth rate (a) and frequency (b) of the SWITG mode as functions of k_y for $\eta_i = \eta_e = 2.0$, $m_i/m_e = 1836$, $T_e/T_i = 1$, $L_n/L_s = 0.025$, $\Omega_e^2/\omega_{pe}^2 = 1$ and $\beta_e = 0$. The solid, dashed, and dotted lines denote the results for $\hat{V}'_0 = 0, 0.5$, and 1.0 , respectively.

the conventional ITG mode. In other words, the \hat{V}'_0 with order v_{ti}/L_n is too small to influence the ETG mode. It is easily understood that the electron nonadiabatic kinetics is dominant for the ETG mode.

The effect of the $\mathbf{E} \times \mathbf{B}$ flow shear on the SWITG mode is shown in Fig. 5. The behavior of the SWITG mode in the presence of sheared $\mathbf{E} \times \mathbf{B}$ flow is same as that of the conventional ITG mode. The initial rise in \hat{V}'_E causes an increase in the growth rate and a decrease in the frequency. The growth rate reaches its maximum values at $\hat{V}'_E \approx 0.013$ – 0.017 depending on different β values. After the frequency approximately reverses its direction, any further increase of \hat{V}'_E causes a decrease in the growth rate. Then, the mode is fully stabilized by a large enough \hat{V}'_E . As we know, the $\mathbf{E} \times \mathbf{B}$ velocity shear affects the mode mainly by changing the value of $\xi_j = (L_s/L_n)(\rho_j/|x|)[\omega/2\omega_{*j} - (x/\rho_j)\hat{V}'_E]$. Since the frequency of the SWITG mode is lower than that of the conventional ITG mode and the radial width of the SWITG mode can be comparable with the conventional ITG mode, the stabilization of the SWITG mode needs much smaller \hat{V}'_E than the stabilization of the ITG mode. For example, at $\beta_e = 0, 0.005$, and 0.05 , the critical \hat{V}'_E values for stabilization of the SWITG mode are $0.068, 0.021$, and 0.036 , respectively, while those for the conventional ITG modes⁴⁵ are $0.17, 0.14$, and 0.075 , respectively. The $\mathbf{E} \times \mathbf{B}$ velocity shear also destroys the symmetric mode structure.

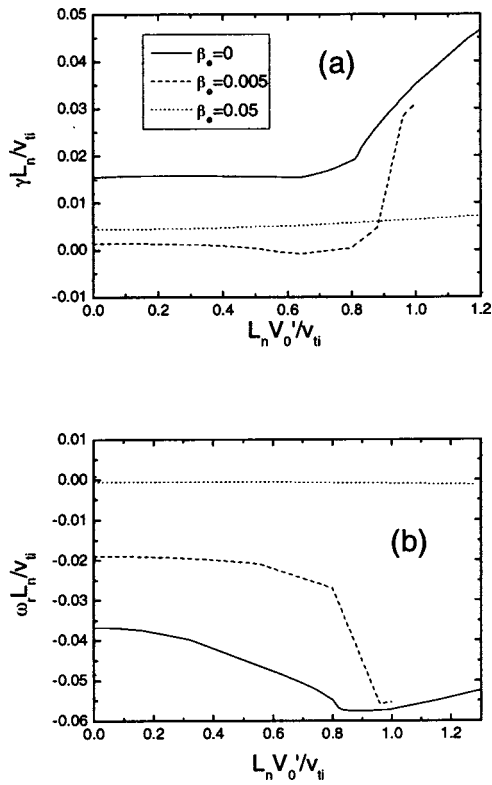


FIG. 2. Mode growth rate (a) and frequency (b) of the SWITG mode as functions of \hat{V}'_0 for $k_y=0.1$. The solid, dashed, and dotted lines denote the results for $\beta_e=0, 0.005$, and 0.05 , respectively. The other parameters are the same as in Fig. 1.

The mode structure shifts toward the $+x$ direction at positive \hat{V}'_E , which is shown in Fig. 6.

The k_y spectra of the SWITG modes for different \hat{V}'_E values are shown in Fig. 7. The shorter wavelength mode is easily stabilized by \hat{V}'_E . The longer wavelength mode can be excited by a finite \hat{V}'_E and then stabilized by a larger enough \hat{V}'_E . This trend can be explained by the fact that the modes at higher k_y regions have higher frequencies.

From the argument of ξ_j , we can also find that magnetic shear strongly influences the \hat{V}'_E effect. Figure 8 shows the mode frequencies and growth rates as functions of L_n/L_s for different \hat{V}'_E values. In the weak shear region, a small \hat{V}'_E can fully stabilize the mode. However, in the stronger shear region a larger \hat{V}'_E is required to stabilize the mode although the growth rate is also depressed by the magnetic shear. This is similar to that for conventional ITG modes in both slab⁴⁵ and toroidal¹⁸ plasmas.

For comparison, Fig. 9 shows the effect of \hat{V}'_E on the ETG mode for different β values. When the V'_E is less than $2v_{ii}/L_n$, the growth rates are weakly changed but the frequencies decrease gradually. When the frequencies become low, any further increase of \hat{V}'_E causes a sharp decrease in the growth rate. The critical \hat{V}'_E values for stabilization of the ETG mode are 4.8, 3.3, and 2.8 at $\beta_e=0, 0.005$, and 0.05 , respectively. These values are also consistent in order with those for electrostatic ETG modes with slightly hollow density profiles.⁴⁸ We emphasize that the critical \hat{V}'_E for the ETG

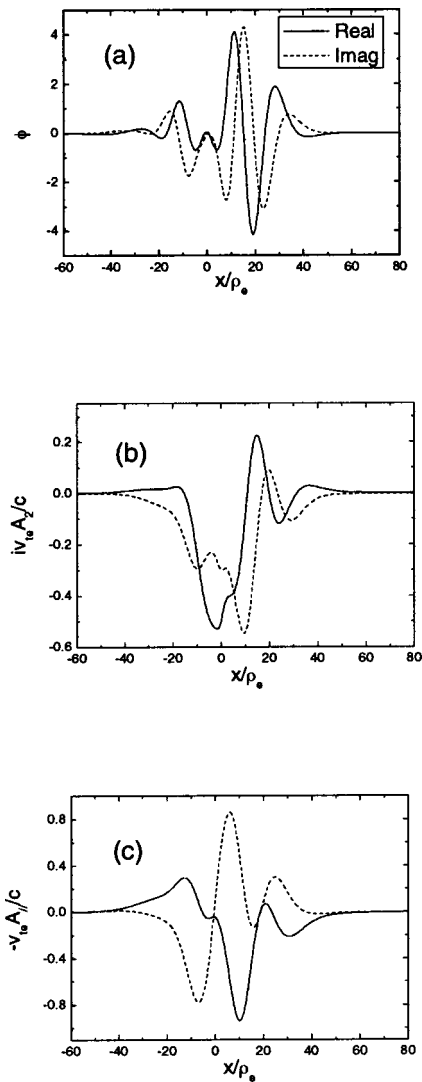


FIG. 3. Mode structure of the SWITG mode for $k_y=0.1$, $\beta_e=0.005$ and $\hat{V}'_0=0.5$: (a) $\phi(x)$ vs x ; (b) $A_2(x)$ vs x ; (c) $A_1(x)$ vs x . The other parameters are the same as in Fig. 1.

mode is much larger than that for the SWITG and conventional ITG modes and is also larger than the observed $\mathbf{E} \times \mathbf{B}$ shearing rate in experiments. This result may provide us evidence to choose a better possible candidate responsible for the anomalous electron transport between the ETG and SWITG instabilities. If the SWITG instability is the only candidate, the $\mathbf{E} \times \mathbf{B}$ shear, which can fully stabilize the SWITG mode, will suppress the high- k turbulence due to the SWITG instability, and trigger the onset of eITBs easily. However, it seems to be inconsistent with the experimental observations.²⁶⁻³¹ In contrast, if the anomalous electron transport is induced by the ETG instabilities, the $\mathbf{E} \times \mathbf{B}$ shear in experiments is not large enough to stabilize the unstable modes alone. Maybe it is the reason that the formation of eITBs is more likely to be triggered by the magnetic shear optimization rather than by the $\mathbf{E} \times \mathbf{B}$ shear enhancement. The ETG mode, in this respect, is more reasonable than the SWITG as the candidate responsible for anomalous electron thermal transport.

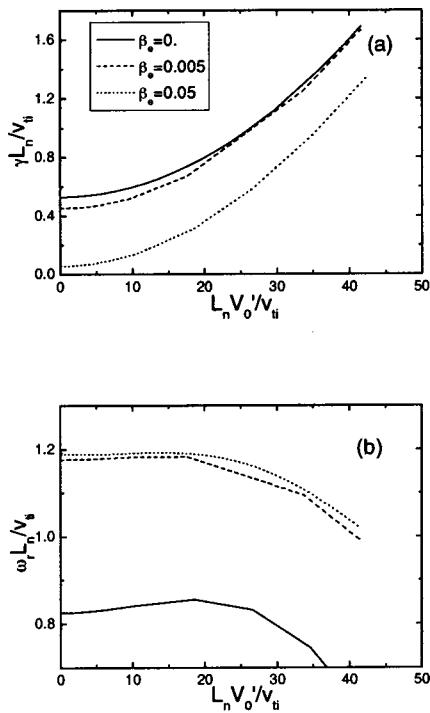


FIG. 4. Mode growth rate (a) and frequency (b) of the ETG mode as functions of \hat{V}'_0 for $k_y=0.8$ and $L_n/L_s=0.1$. The other denotations and parameters are the same as in Fig. 1.

IV. CONCLUSIONS AND DISCUSSION

In this paper, the effects of flow shear on the SWITG modes are investigated. Usually, a strong parallel velocity

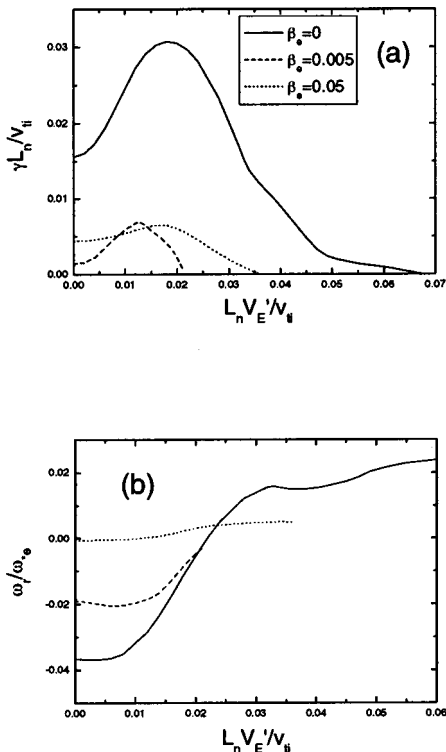


FIG. 5. Mode growth rate (a) and frequency (b) of the SWITG mode as functions of \hat{V}'_E for $k_y=0.1$. The solid, dashed, and dotted lines denote the results for $\beta_e=0, 0.005,$ and $0.05,$ respectively. The other parameters are the same as in Fig. 1.

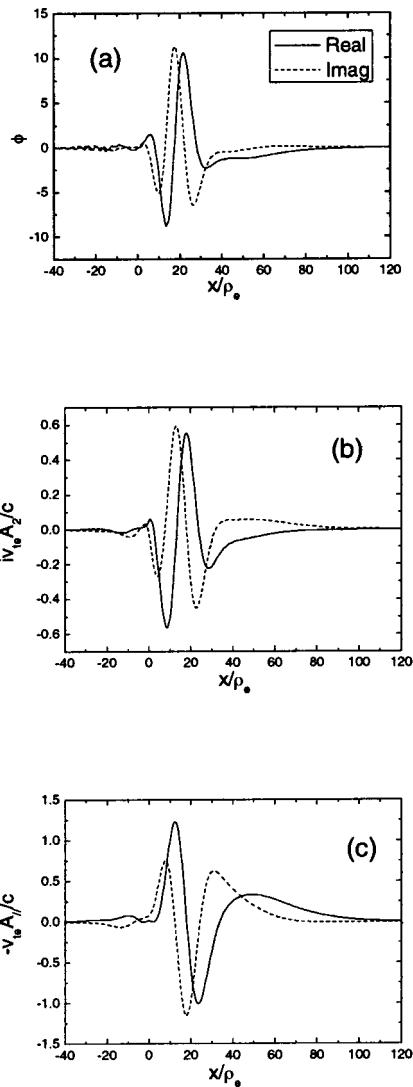


FIG. 6. Mode structure of the SWITG mode for $k_y=0.1, \beta_e=0.005$ and $\hat{V}'_E=0.02$: (a) $\phi(x)$ vs x ; (b) $A_2(x)$ vs x ; (c) $A_{||}(x)$ vs x . The other parameters are the same as in Fig. 1.

shear is destabilizing, while the destabilizing effect is depressed or even turned into the stabilizing effect as k_y increases from $|\rho_i|^{-1}$ to ρ_e^{-1} . Also, the effect of the parallel velocity shear is weakened by high β . The effect of the **EXB** velocity shear on the SWITG modes is similar to that on the conventional ITG mode. The growth rate increases in the low V'_E region but a large enough V'_E can completely stabilize the mode. At a weak magnetic shear, the stabilizing effect of the **EXB** velocity shear is highly strengthened. With lower frequencies, the SWITG modes need lower V'_E to be stabilized than the conventional ITG modes do.

The effects of sheared flows on the ETG modes are also studied using the same code. Since the electron kinetics is dominant for the ETG mode, a very strong flow shear is needed to influence the stabilization properties of the ETG modes. In detail, the V'_0 with order v_{ti}/L_n is too small to influence the ETG mode and the critical V'_E values for stabilization of the ETG modes are also much larger than those for the SWITG and conventional ITG modes.

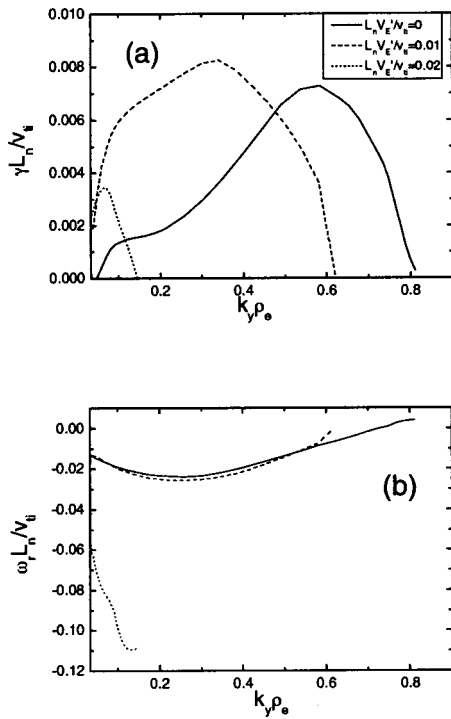


FIG. 7. Mode growth rate (a) and frequency (b) of the SWITG mode as functions of \hat{V}'_E for different $L_n/L_s=0.025$ (solid), 0.05 (dashed), and 0.075 (dotted), respectively. $\beta_e=0.005$, $k_y=0.1$ and the other parameters are the same as in Fig. 1.

Recent work⁴³ indicates that the growth rate of the ETG mode is about 20 times larger than that of the SWITG mode, while the radial width of the latter is about ten times larger than that of the ETG mode. Therefore, the turbulence trans-

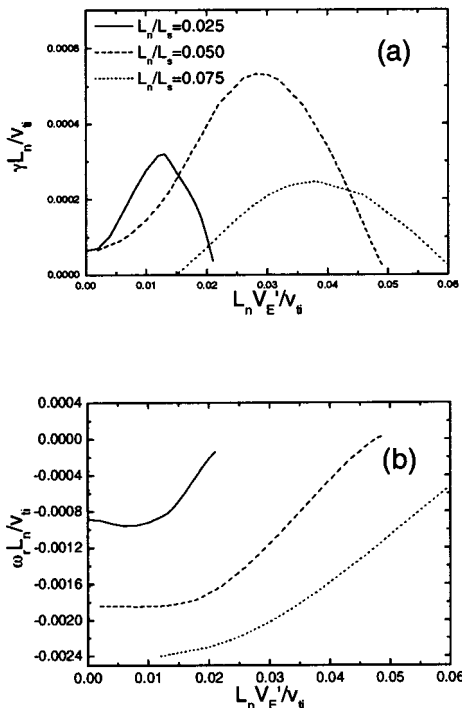


FIG. 8. Mode growth rate (a) and frequency (b) of the SWITG mode as functions of k_y for different $\hat{V}'_E=0$ (solid), 0.01 (dashed), and 0.02 (dotted), respectively. $\beta_e=0.005$ and the other parameters are the same as in Fig. 1.

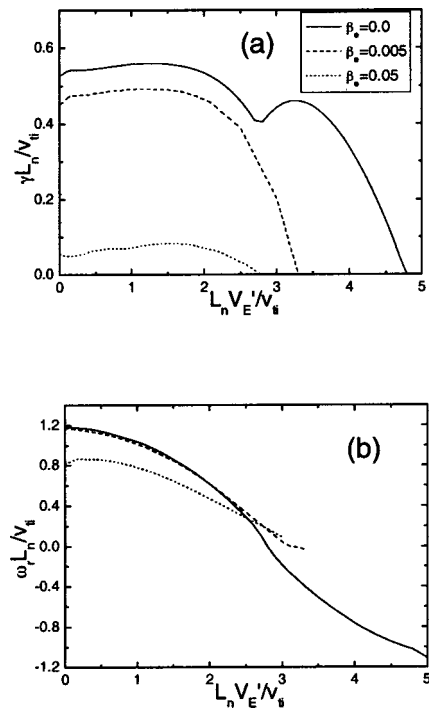


FIG. 9. Mode growth rate (a) and frequency (b) of the ETG mode as functions of \hat{V}'_E for $k_y=0.8$ and $L_n/L_s=0.1$. The parameters and denotations are the same as in Fig. 1.

port induced by these short wavelength modes may be much higher than that by ETG turbulence. It is expected that the SWITG mode could contribute much to electron transport. However, in present work, we find that the SWITG mode is easily stabilized by the $\mathbf{E} \times \mathbf{B}$ velocity shear, especially in the weak magnetic shear region. Therefore, if the SWITG mode were responsible for anomalous electron transport, the $\mathbf{E} \times \mathbf{B}$ shear should be an effective trigger of the eITBs. It seems to be inconsistent with the experimental observations although there is no direct comparison between the $\mathbf{E} \times \mathbf{B}$ shear rate and the growth rate of the SWITG instability. In contrast, the ETG mode seems to be more reasonable than the SWITG as the candidate responsible for anomalous electron thermal transport.

However, it is noted that not all tokamaks observed stiffness in electron temperature profile.^{49,50} On the other hand, some ITG-TEM-based (not ETG-based) transport models have successfully simulated the experimental results with electron heating.⁵¹ It implies that the mechanism of electron transport may be not universal. Those complicated transport phenomena for electrons need further research, especially with the collaboration of profile control, diagnostics, theoretical analyses, and simulations.

ACKNOWLEDGMENTS

We wish to acknowledge helpful discussions with Professor K. Itoh at National Institute for Fusion Science.

This work is supported by Improving Tsinghua to Top-ranking University Fund and National Science Foundation of China, Grant Nos. 10375089 and 10135020.

- ¹K. Itoh and S.-I. Itoh, *Plasma Phys. Controlled Fusion* **38**, 1 (1996).
- ²B. Coppi, M. N. Rosenbluth, and R. Z. Sagdeev, *Phys. Fluids* **10**, 582 (1967).
- ³R. Linsker, *Phys. Fluids* **24**, 1485 (1981).
- ⁴Y. C. Lee, J. Q. Dong, P. N. Guzdar, and C. S. Liu, *Phys. Fluids* **30**, 1331 (1987).
- ⁵A. Jarmen, P. Anderson, and J. Weiland, *Nucl. Fusion* **27**, 941 (1987).
- ⁶W. Horton, B. G. Hong, and W. M. Tang, *Phys. Fluids* **31**, 2971 (1988).
- ⁷T. S. Hahm and W. M. Tang, *Phys. Fluids B* **1**, 1185 (1989).
- ⁸L. Chen, S. Briguglio, and F. Romanelli, *Phys. Fluids B* **3**, 611 (1991).
- ⁹J. Y. Kim, W. Horton, and J. Q. Dong, *Phys. Fluids B* **5**, 4030 (1993).
- ¹⁰M. A. Beer and G. W. Hammett, *Phys. Plasmas* **3**, 4046 (1996).
- ¹¹W. W. Lee and R. A. Santoro, *Phys. Plasmas* **4**, 169 (1997).
- ¹²F. M. Levinton, M. C. Zarnstorf, S. H. Batha *et al.*, *Phys. Rev. Lett.* **75**, 4417 (1995).
- ¹³E. J. Strait, L. L. Lao, M. E. Mauel *et al.*, *Phys. Rev. Lett.* **75**, 4421 (1995).
- ¹⁴H. Shirai and JT-60 Team, *Phys. Plasmas* **5**, 1712 (1998).
- ¹⁵C. Gormezano, Y. F. Baranov, C. D. Challis *et al.*, *Phys. Rev. Lett.* **80**, 5544 (1998).
- ¹⁶K. H. Burrell, *Phys. Plasmas* **4**, 1499 (1997).
- ¹⁷M. Artun and W. M. Tang, *Phys. Fluids B* **4**, 1102 (1992).
- ¹⁸J. Q. Dong and W. Horton, *Phys. Fluids B* **5**, 1581 (1993).
- ¹⁹H. Biglari, P. H. Diamond, and P. W. Terry, *Phys. Fluids B* **2**, 1 (1990).
- ²⁰T. S. Hahm and K. H. Burrell, *Phys. Plasmas* **2**, 1648 (1995).
- ²¹A. S. Ware, P. W. Terry, P. H. Diamond *et al.*, *Plasma Phys. Controlled Fusion* **38**, 1343 (1996).
- ²²K. Itoh and S.-I. Itoh, *Plasma Phys. Controlled Fusion* **38**, 1 (1996).
- ²³E. Mazzuato, S. H. Batha, M. Beer *et al.*, *Phys. Rev. Lett.* **77**, 3145 (1996).
- ²⁴B. W. Stallard, C. M. Greenfield, G. M. Staebler *et al.*, *Phys. Plasmas* **6**, 1978 (1999).
- ²⁵G. D. Conway, D. N. Borba, B. Alper *et al.*, *Phys. Rev. Lett.* **84**, 1463 (2000).
- ²⁶P. Buratti, E. Barbato, G. Bracco *et al.*, *Phys. Rev. Lett.* **82**, 560 (1999).
- ²⁷G. T. Hoang, C. Bourdelle, X. Garbet *et al.*, *Phys. Rev. Lett.* **84**, 4593 (2000).
- ²⁸R. C. Wolf, S. Gunter, F. Leuterer *et al.*, *Phys. Plasmas* **7**, 1839 (2000).
- ²⁹K. A. Razumova, V. F. Andreev, A. A. Borshchegovskii *et al.*, *Plasma Phys. Controlled Fusion* **45**, 1247 (2003).
- ³⁰C. M. Greenfield, K. H. Burrell, T. A. Casper *et al.*, in *Proceeding of 27th EPS Conference on Controlled Fusion and Plasma Physics*, Budapest 2000, edited by K. Szegő, T. N. Todd, and S. Zoletnik (European Physical Society, Petit-Lancy, 2000), ECA Vol. 24B, p. 544.
- ³¹A. Fujisawa, H. Iguchi, T. Minami *et al.*, *Phys. Plasmas* **7**, 4102 (2000).
- ³²M. A. Beer, G. W. Hammett, G. Rewoldt *et al.*, *Phys. Plasmas* **4**, 1499 (1997).
- ³³R. E. Waltz, G. M. Staebler, W. Dorland *et al.*, *Phys. Plasmas* **4**, 2482 (1997).
- ³⁴F. Romanelli and F. Zonca, *Phys. Fluids B* **5**, 4081 (1993).
- ³⁵X. Garbet, C. Bourdelle, and G. T. Hoang, *Phys. Plasmas* **8**, 2793 (2001).
- ³⁶J. Q. Dong, W. Horton, and Y. Kishimoto, *Phys. Plasmas* **8**, 167 (2001).
- ³⁷F. Ryter, C. Angioni, M. Beurskens *et al.*, *Plasma Phys. Controlled Fusion* **43**, A323 (2001).
- ³⁸Y. Idomura, M. Wakatani, and S. Tokuda, *Phys. Plasmas* **7**, 2456 (2000).
- ³⁹F. Jenko, W. Dorland, M. Kotschereuther, and B. N. Rogers, *Phys. Plasmas* **7**, 1904 (2000).
- ⁴⁰J. Q. Dong, H. Sanuki, K. Itoh, and L. Chen, *Phys. Plasmas* **9**, 4699 (2002).
- ⁴¹J. Q. Dong, G. D. Jian, A. K. Wang, H. Sanuki, and K. Itoh, *Nucl. Fusion* **43**, 1185 (2003).
- ⁴²A. I. Smolyakov, M. Yagi, and Y. Kishimoto, *Phys. Rev. Lett.* **89**, 125005 (2002).
- ⁴³Z. Gao, H. Sanuki, K. Itoh, and J. Q. Dong, *Phys. Plasmas* **10**, 2831 (2003).
- ⁴⁴A. Hirose, M. Elia, A. I. Smolyakov, and M. Yagi, *Phys. Plasmas* **9**, 1659 (2002).
- ⁴⁵Z. Gao, J. Q. Dong, G. J. Liu, and C. T. Ying, *Phys. Plasmas* **10**, 774 (2003).
- ⁴⁶G. Ganguli, Y. C. Lee, and P. J. Palmadesso, *Phys. Fluids* **31**, 823 (1988).
- ⁴⁷H. Sanuki, *Phys. Fluids* **27**, 2500 (1984).
- ⁴⁸J. Q. Dong, H. Sanuki, and K. Itoh, *Phys. Plasmas* **8**, 3635 (2001).
- ⁴⁹J. C. DeBoo, M. E. Austin, R. V. Bravenc *et al.*, in *Proceeding of 29th EPS Conference on Controlled Fusion and Plasma Physics*, Montreux, 2002, edited by R. Behn and C. Varandas (European Physical Society, Petit-Lancy, 2002), ECA Vol. 26B, p. 2064.
- ⁵⁰W. Suttrop, R. Budny, J. G. Cordey *et al.*, in *Proceeding of 28th EPS Conference on Controlled Fusion and Plasma Physics*, Funchal, 2001, edited by C. Silva, C. Varandas, and D. Campbell (European Physical Society, Petit-Lancy, 2001), ECA Vol. 25A, p. 989.
- ⁵¹G. Tardini, A. G. Peeters, G. V. Pereverzev *et al.*, *Nucl. Fusion* **42**, L11 (2002).